Ocean Engineering 110 (2015) 116–125

Contents lists available at ScienceDirect

Ocean Engineering

journal homepage: www.elsevier.com/locate/oceaneng

Performance of CZT-assisted parallel combinatory multicarrier Frequency-Hopping Spread Spectrum over shallow underwater acoustic channels

Fang Xu *, Chaowu Zhan, Yongjun Xie, Deqing Wang

The Key Laboratory of Underwater Acoustic, Communication and Marine Information Technology, Xiamen University, Xiamen, Fujian 361005, China

ARTICLE INFO

Article history:
Received 21 February 2014
Accepted 1 October 2015
Available online 26 October 2015

Keywords:
Underwater acoustic
Parallel combination
Frequency-Hopping Spread Spectrum
Multicarrier
Chirp-Z Transform

ABSTRACT

A Parallel Combinatory multicarrier Frequency-Hopping Spread Spectrum (PC/MC-FHSS) Underwater Acoustic (UWA) communication system combined with a Chip-z Transform (CZT) method is proposed in this paper. One of the advantages of the PC/MC-FHSS system is its ability to resist fading and random narrowband interference during transmission over the UWA channel. Another benefit is increasing the data rate of the system. Results of computer simulations and pool experiments prove that the proposed CZT-assisted PC/MC-FHSS communication system exhibits greater BER performance and higher data rate than those of the traditional FHSS system and the PC/MC-FHSS system. Outfield experiments carried out in Xiamen Port show that the BER performance of the system is on the order of 10^{-3}, when the data rate is up to 469 bps and the distances of the communication systems is 10 km.

1. Introduction

The Underwater Acoustic (UWA) channel is one of the most challenging channels for communication. The prominent characteristics of the UWA channel are frequency-dependent path loss, multipath propagation, and low speed of sound (Stojanovic, 2008). Specially, frequency-dependent path loss leads to limited bandwidth that can be used especially for long range communications. Inter-symbol Interference (ISI) caused by multipath underwater transmission is so serious that it always extends over tens or even hundreds of milliseconds (ms), depending on the distance of the communications (Stojanovic, 2008). Because the velocity of sound in water is only about 1500 m/s, any relative motion of the transmitter or the receiver, or even surface waves and undercurrents cannot cause negligible Doppler shifting and Doppler Spread. All these facts dramatically limit the achievable data rate and the performance of the UWA communication systems. Recently, much research has been carried out covering different aspects of UWA communications, including UWA channel modeling, modulation schemes, signal detection, equalization, etc (Geng and Zielinski, 1995; Stojanovic and Preisig, 2009; Lam and Ormondroyd, 1998; Hu and Jiao, 2005; Stojanovic et al., 1993). For short range communications, multicarrier schemes, such as Orthogonal Frequency Division Multiplexing (OFDM), have been widely studied (Wang et al., 2010). The experimental results show that the OFDM data rate is on the order of kilo bits per second (kbps), while the BER is 10^{-5} when the communication distance is 1 km. For long range communication, if one considers the inherent drawbacks of multicarrier modulation (high peak-to-average power ratio (PAPR)) and the frequency selective fading and deep fading of the UWA channel, then the SNR of the subcarrier on the receiver side decreases rapidly making the performance of the system unacceptable. It seems that a single-carrier (SC) scheme, such as the Frequency-Hopping Spread Spectrum (FHSS) system, is a suitable candidate for long range transmission. On the one hand, FHSS signals are highly resistant to narrow band interference. Especially when they are used in the military, they are highly resistant to deliberate jamming and are difficult to intercept. On the other hand, selective frequency fading and deep fading coexist during transmission in UWA channels. Therefore, in this scenario, when FHSS is applied, the system is more robust. A FHSS-4FSK communication system has been studied (Tao et al., 2010; Shu and Shen, 2012). Sea experiments have been conducted at different ranges, i.e. 3 km and 6 km, respectively. The data rate is 200 bps, while the BER of the system is about 10^{-2}. Research on the different modulation types of FHSS-MFSK systems has been performed (Liu et al., 2012). Pool experiments have been conducted to

* Corresponding author.
E-mail addresses: xufang@xmu.edu.cn (F. Xu), zhanchaowu517@gmail.com (C. Zhan), xyj@xmu.edu.cn (Y. Xie), deqing@xmu.edu.cn (D. Wang).

http://dx.doi.org/10.1016/j.oceaneng.2015.10.005
0029-8018/

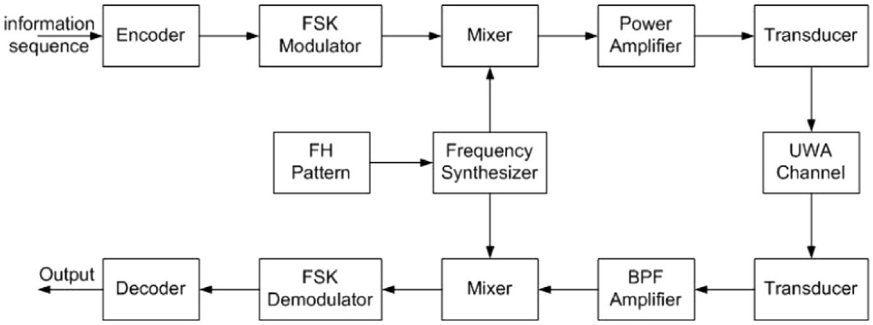

Fig. 1. Block diagram illustrating the general structure of FHSS communication systems.

compare their advantages and disadvantages. In Wang et al. (2006) experimental results for a short range (3 km) FHSS communication system were proposed. The BER of the system is about 10^{-3} when the SNR is only -20 dB, but the data rate is 2 bps. A Frequency Hopping Multiple Access (FHMA) acoustic communication system also has been studied (Zhao and Guo, 2010), where frequency hopping sequence orthogonality was utilized to distinguish the different access. Simulation results show that the orthogonality of frequency hopping sequence is feasible to be used as a access method.

As for long range UWA communications, especially for distances longer than 10 km, there were few papers which focused on this topic. Huang et al. (2005) proposed a MFSK-NDPSK system which combined the frequency and phase modulation. The results of the lake experiments showed that the BERs of this underwater acoustic communication system were on the order of the 10^{-2} before Turbo decoding when the distance of the communication was 25 km and the depth of the water was about 50–100 m. Another system called SD-JFPM was proposed by the same research group (Ran et al., 2008). The paper showed that this underwater acoustic communication system also can work well in long distance, such as 25 km in a lake where the depth of it was about 50–100 m. The BERs of the proposed system were also on the order of the 10^{-2} before Turbo decoding. We had proposed a Parallel Combinatory MultiCarrier FHSS (PC/MC-FHSS) system (Chaowu Zhan, 2013), and the outfield experiment results showed that this system can work well in shallow water at the range of 10 km and 15 km. In this paper, further research has been done. New methods such as a Chirp-Z Transform (CZT) detection in very limited bandwidth was employed to increase the data rate of the proposed UWA system as well as to enhance the BER performance of the UWA communication system. The proposed CZT-assisted PC/MC-FHSS communication systems was verified by simulations, pool experiments and outfield experiments in Xiamen Port. The results of the outfield experiment showed that when the communication distance was longer than 10 km, the BER was on the order of 10^{-3}, while the data rate was 469 bps.

The remainder of this paper is organized as follows: Section 2 investigates the theory and structure of the PC/MC-FHSS. Parameters of the system are also given in this section. Section 3 presents computer simulation and an analysis of the results. Section 4 gives experimental results of the pool, and tests several schemes. Section 5 details and analyzes the outfield results, leading to our conclusions in Section 6.

2. Parallel combinatory multicarrier FHSS UWA system model and parameters design

Two of the problems often met when designing UWA communication systems are the frequency-selective fading caused by multipath propagation and the deep fading due to the absorption of signals by sea water, sea bottom as well as dramatic changes of the topography of seabed. Therefore, after a long distance transmission, the SNR of received signals is usually very low. Hence, in UWA communications, it is highly challenging to improve both reliability and data rate at the same time. It is well-known that the inherent characteristics of FH provide the FHSS systems the capability to mitigate the effect of both frequency-selective fading and absorption-generated deep fading, especially, when fast FH (FFH) is employed. However, limited by the bandwidth available and the large transmission delay of UWA channels, in the conventional FHSS communication systems, the attainable data rate is usually very low and not enough to provide the services requiring high data rates. In this section, we first provide an introduction for the conventional SC- and MC-FHSS systems. Based on their principles, then, we propose the PC/MC FHSS communication scheme. Finally, the parameters of the proposed system are addressed.

Table 1
Parameters of SC-FHSS systems.

Symbol interval	10 ms	Data rate	200 bps
Bandwidth	3.2 kHz	Hopping mode	Fast hopped
Modulation	4FSK	Detection	Noncoherent detection

2.1. Conventional FHSS systems and parameter design

In FHSS systems, the frequency of a transmitted signal varies according to a predefined FH pattern and hops from one to another within the available frequency bands. In other words, FH signals belong to the class of multi-frequency shift keying signals in the time domain. In FHSS systems, it is very difficult to maintain phase continuity, which makes phase estimation highly challenging, hence, non-coherent detection is often employed by the receivers.

The schematic structure of a FHSS communication system can be shown as Fig. 1, where the upper part for the transmitter and the lower part for the receiver are connected by the UWA channel. As shown in Fig. 1, the transmitter consists of an encoder for error-control, a FSK modulator for data modulation, a frequency mixer for implementing FH with the aid of a frequency synthesizer supported by a unique FH pattern. Finally, signals are transmitted via a transducer after power amplification. At the receiver, the inverse operations to those employed by the transmitter are typically carried out, in order to detect the received information. For the sake of comparison, in this paper, both SC- and MC-FHSS systems are considered. The difference between these two FHSS schemes might be the implementation of the FSK modulator and the FH. Specifically, in a SC-FHSS system, information is first FSK modulated and then frequency hopped over the entire available frequency band. Considering the characteristics of shallow UWA channels and the limited frequency bandwidth available, in our studies, the parameters used by the SC-FHSS system are set

according to that as shown in Table 1. As for the MC-FHSS system, in our studies, the whole frequency band available is first divided into two parts, namely the high-frequency part and low-frequency part. Then, each part is further divided into K groups of each group having 8 sub-bands supported by the corresponding subcarriers. At the transmitter, after the serial to parallel (S–P) conversion, information bits are modulated on K subcarriers, each of which is selected from one of the K groups. Furthermore, the transmitted frequency hops between the two parts at the symbol rate. In summary, the parameters set for the MC-FHSS systems are shown in Table 2.

2.2. PC/MC-FHSS communication system and parameter design

Because the bandwidth of UWA communication channels is very limited and UWA channels experience frequency-selective and deep fading, in this paper, a CZT-assisted PC/MC-FHSS system is proposed, which is capable of taking the advantages of the PC/MC-FHSS system and the CZT detection method to increase the data rate of communication. In Chaowu Zhan (2013), we extended the parallel combinatory direct-sequence spread spectrum (PC/DS-SS) (Zhu and Sasaki, 1991) to the MC-FHSS system, forming the PC/MC-FHSS. In our PC/MC-FHSS system, R out of M subcarriers are selected for transmission of every symbol.

Definition 1. Suppose a R-combination of a set with M different elements is denoted as ${C_M}^R$, where N_a is the index of one combination $(a_1, a_2, \ldots, a_R)$ and N_b is the index of another combination $(b_1, b_2, \ldots, b_R)$. If R elements of these two combinations satisfy

$$\begin{cases} a_i = b_i, & i = 1, 2, \ldots, j-1 \\ a_j < b_j, & j \in (1, 2, \ldots, R),\ j \le R \end{cases}$$

then, $N_a < N_b$. This sequence is defined as an ordered sequence.

Two theorems are given below (Guo et al., 2007).

Theorem 1. *If N_a is the index of one combination of ${C_M}^R$, where $C_M^R = M!/(R!(M-R)!)$, then all the elements $a_i (1 \le i \le R)$ of this combination are determined by*

$$\min_{\{a_i\}} C_{M-a_i}^{R-i+1} \le C_M^R - N_a - \sum_{t=1}^{i-1} C_{M-a_i}^{R-t+1} \tag{1}$$

where $\min_{\{a_i\}}$ is the minimum of a_i.

Theorem 2. *The index number of one combination $(a_1, a_2, \ldots, a_R)$ of ${C_M}^R$ is determined by*

$$N_a = a_R - a_{R-1} + \sum_{t=0}^{R-2} (C_{M-a_t}^{R-t} - C_{M+1-a_{t+1}}^{R-t}) \tag{2}$$

where $a_0 = 0$.

Theorem 1 shows that when the index of one combination ${C_M}^R$ is known, the elements of this combination are uniquely determined. Theorem 2 shows that when the elements of one combination are chosen, its index is also uniquely fixed.

The block diagram of the proposed PC/MC-FHSS system is shown in Fig. 2, which is similar as Fig. 1, except the modulation/demodulation. Specifically, as shown in Fig. 2, after the encoding and S/P conversion, K bits of information are sent to the subcarrier mapping module, where R of the M subcarriers are chosen for conveying the information. As there are ${C_M}^R$ unique combinations, when choosing R out of the M different elements, we can transmit $K = \lfloor \log_2 C_M^R \rfloor$ bits per symbol. As shown in Fig. 2, our PC/MC-FHSS employs FH, in order to mitigate the fading. However, as the bandwidth for UWA communications is very limited, the FH in the PC/MC-FHSS system is operated only on two frequency sub-bands, $\{f_{c1}, f_{c2}\}$, and the subcarriers are transmitted on these two frequency sub-bands under the control of a FH pattern, which varies at the symbol rate. Finally, after the power amplification, the mixed signal is transmitted by the transducer. The transmitted signal for the jth symbol can be written as

$$s(t) = \sum_{j=0}^{N-1} P_{T_0}(t - jT_0) \times \left(\sum_{i=1}^{R} \cos(2\pi f_i^{(j)} t) \right) \cos(2\pi f_{cj} t) \tag{3}$$

where $f_i^{(j)}, i = 1, 2, \ldots, R$ are subcarrier frequencies, which are determined by the transmitted information of the jth symbol, $f_{cj} \in \{f_{c1}, f_{c2}\}$ denotes the carrier frequency, which is determined by the FH pattern, N is the length of a block of data symbols, and $P_{T_0}(t)$ denotes a rectangular waveform, which is defined as $P_{T_0}(t) = 1$, when $0 < t \le T_0$ and $P_{T_0}(t) = 0$, otherwise.

After transmission of the signal in the form of 3 over a UWA channel with L paths, the received signal can be presented as

$$r(t) = \sum_{l=1}^{L} \alpha_l s(t - \tau_l) + n(t) \tag{4}$$

where α_l and τ_l denote the channel gain and the propagation delay of the lth multipath, respectively, while $n(t)$ is Gaussian noise added at the receiver, which is assumed to have the single-sided

Table 2
Parameters of MC-FHSS systems

Symbol interval	25 ms	Data rate	360 bps
Bandwidth	3.84 kHz	Hopping mode	Slow hopped
No. of groups per part	3	Detection	Noncoherent detection

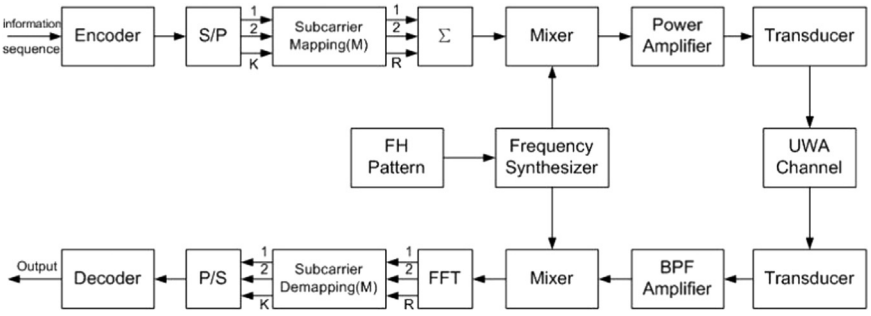

Fig. 2. Schematic block diagram of the PC/MC-FHSS systems.

power spectrum density (PSD) N_0. In this paper, we assume that the fading is slow relative to the symbol rate. Hence, α_l remains constant during one symbol interval.

As shown in Fig. 2, after the BPF and FH dehopping, the receiver of this signal consists of a mixer followed by n noncoherent detection module where a Discrete Fourier Transformation (DFT) is employed to search the spectra of the signal in order to determine the combinatory multicarrier frequencies. And according to the PC theory discussed above, K bits are demodulated. Here we replace DFT by Fast Fourier Transform (FFT) because of its fast and efficient algorithm. The data rate of this PC/MC-FHSS system is expressed as

$$R_b = \frac{K}{T_0} = \frac{\lfloor \log_2 C_M^R \rfloor}{T_0} (bit/s) \tag{5}$$

where $K = \lfloor \log_2 C_M^R \rfloor$, $\lfloor x \rfloor$ represents the largest integer not larger than x. M is the subcarriers available in this system and $C_M{}^R$ is a R-combination of a set M. T_0 is the symbol interval.

Since the bandwidth of the underwater acoustic channel is very limited, especially for the long range, for example, the bandwidth of the transducers employed in our experiments is only about 4 KHz, i.e. 4–8 KHz. The bandwidth should be divided into two sub-bandwidth to support frequency hopping in our system, the available bandwidth is further limited. Also we have to consider the non-coherent detection at the receiver side and the frequencies applied at sender side should have enough protective spacing. Moreover, the data rate of the communication system is the major issue to be considered. As shown in (5), the selection of the R and M directly determine the data rate of the proposed system. We select five sets of parameters to verify the performance of the proposed system over different data rate, different bandwidth and different hopping mode. These parameters are shown in Tables 3 and 4, respectively.

As shown in Table 4, compared with other schemes, the scheme 2 occupies less bandwidth that can achieve a data rate of 400 bps. When compared with a SC-FHSS system (as shown in Table 1), we observe that when the signal occupies the same bandwidth, i.e. 3.2 kHz, the data rate of the traditional FHSS system is only 200 bps, whereas the data rate of the scheme 2 is 400 bps. Additionally, the symbol interval of the traditional FHSS system is 10 ms, while that of the scheme 2 is 25 ms, resulting in that the former being more vulnerable to serious ISI than the latter. A comparison is also made between the traditional multicarrier and PC/MC-FHSS systems. When the symbol interval is the same, that is 25 ms (see Tables 2 and 4) the data rate of the scheme 2 is higher than the traditional one, although the proposed system occupies less bandwidth. All the above characteristics show that the PC/MC-FHSS system is far superior to the traditional one.

Table 3
Parameters of PC/MC-FHSS systems.

Bandwidth	4–8 kHz	Hopping number	2
Hopping mode	slow /or fast hopped	Demodulation	Noncoherent detection

Table 4
Parameters of five sets of schemes.

Scheme	Symbol interval (ms)	R/M	Data rate (bps)	Bandwidth (kHz)	Hopping mode
1	50	2/46	200	3.68	Slow hopped
2	25	3/20	400	3.2	Slow hopped
3	40	4/37	400	3.7	Slow hopped
4	50	5/44	400	3.52	Slow hopped
5	25.6	3/20	391	3.28	Fast hopped

2.3. A CZT-assisted PC/MC-FHSS communication system and parameters design

In regard to the limited bandwidth of the UWA communication and the requirement for a higher data rate, it is a challenge to increase the data rate of the proposed system further and at the same time maintain its robust performance under these circumstances. In this subsection, CZT method is utilized to analyze the spectra of the received signals instead of DFT. The CZT algorithm is a supplement of the DFT algorithm, and it can achieve high frequency resolution when being applied to detect frequency of the signal. Suppose that the points z_k in the z-plane fall on an arc which begins at a point $z_0 = r_0 e^{j\theta_0}$ and spirals either in toward the origin or out away from the origin, where r_0 is the circle's radius and θ_0 is the initial phase angle. Then the points $\{z_k\}, k = 0, 1, \ldots, N-1$ are defined as

$$z_k = z_0 (r_0 e^{j\phi_0})^k = r_0 e^{j\theta_0} (r_0 e^{j\phi_0})^k \tag{6}$$

where R_0 is the Spiral's stretch rate and ϕ_0 is the angle interval among sampling points. And the CZT algorithm can be expressed as

$$X(z_k) = \sum_{n=0}^{N-1} x(n) z_k^{-n} = \sum_{n=0}^{N-1} x(n) (r_0 e^{j\theta_0})^{-n} (r_0 e^{j\phi_0})^{-nk} \tag{7}$$

where if $r_0 = 1$ and $r_0 = 1$, the contour is an arc of the unit circle. The initial phase θ_0 can be changed to probe different frequencies. It is clear that DFT is only a special case of CZT where $r_0 = 1$, $r_0 = 1$ and $\theta_0 = 0$ (Rabiner et al., 1969).

Based upon the above theory, there are many more frequencies to be set in the transmitter. W data bits are converted to parallel signal, where $W = L + K$. The W bits are divided into the following two parts: (1) The first L bits specify the initial phase θ_0 of CZT to determine M subcarriers (see Section 2.2). So, the subcarrier intervals of the M subcarriers of DFT are divided into 2^L parts. (2) The second K bits specifies the R subcarriers in the proposed PC/MC-FHSS system. Spectrum analysis technology is also used in the receiver to restore the data. Combining CZT technology and PC theory, we propose a CZT-assisted PC/MC-FHSS system. The block diagram of the system is shown in Fig. 3 and the parameters of the system are shown in Table 5.

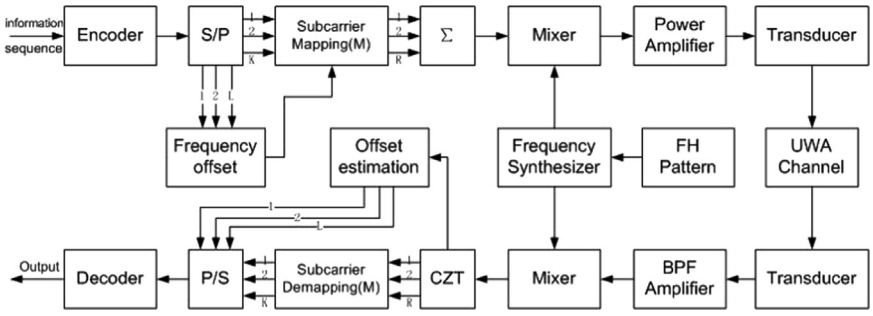

Fig. 3. Schematic block diagram of the CZT-assisted PC/MC-FHSS communication systems.

Table 5
Parameters of CZT-assisted PC/MC-FHSS system.

Symbol interval	25.6 ms	Data rate	469 bps
Bandwidth	3.25 kHz	Hopping mode	Slow hopped
L	2	R	3
M	20	Detection	Noncoherent detection

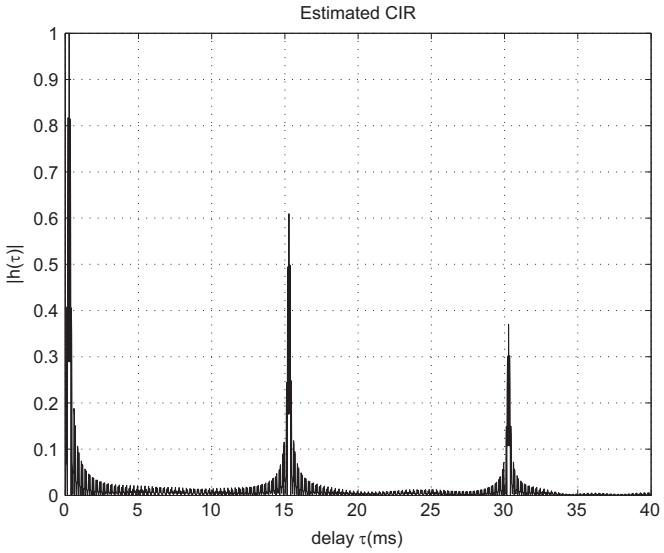

Fig. 4. The CIR of the multipath fading channel, where $\tau_1 = 15$ ms and $\tau_2 = 30$ ms.

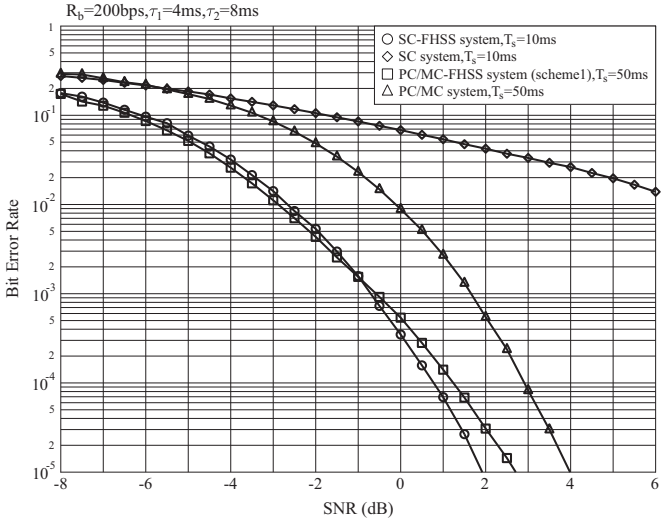

Fig. 5. BER performance comparison of single-carrier communication system and PC multicarrier communication system, with frequency-hopping and non-frequency-hopping, when communicating over 3-path fading channel, where $\tau_1 = 4$ ms and $\tau_2 = 8$ ms.

As shown in Table 5, when compared with the scheme 2 in Table 4, the bandwidth increased by only 50 Hz, but the data rate is 69 bps higher than that of scheme 2. And the remainder of the parameters are similar to those in the scheme 2 system.

3. Computer simulation and result analysis

In this section, we provide a range of simulation results to illustrate the achievable performance of the proposed PC/MC-FHSS system and the CZT-assisted PC/MC-FHSS system. For simplicity, a

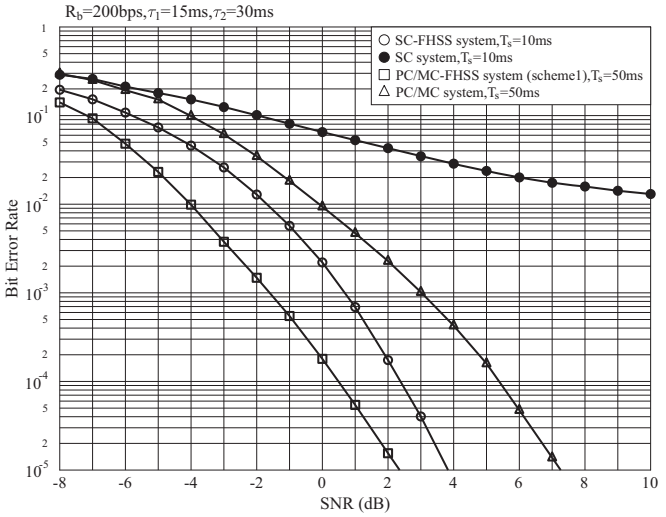

Fig. 6. BER performance comparison of single-carrier communication system and PC multicarrier communication system, with frequency-hopping and non-frequency-hopping, when communicating over 3-path fading channel, where $\tau_1 = 15$ ms and $\tau_2 = 30$ ms.

UWA multipath channel in the simulation is modeled as a 3-path frequency-selective fading channel, and the Channel Impulse Response (CIR) is given as

$$h(t) = \sum_{l=0}^{L-1} \sqrt{P_l}\delta(t-\tau_l) \tag{8}$$

where its power delay spectrum has a negative exponential distribution expressed as

$$P_l = \exp(-\tau_l/\tau_{mean}) \tag{9}$$

where τ_l is the relative delay time of lth path, and τ_{mean} is the mean of delay. In order to verify the BER performance of the proposed system working over different frequency selective fading channel, two sets of channel parameters are chosen, i.e. small delays ($\tau_1 = 4$ ms and $\tau_2 = 8$ ms) and large delays ($\tau_1 = 15$ ms and $\tau_2 = 30$ ms), respectively. Fig. 4 shows the CIR of the multipath fading channel given in (8). Suppose that the transmitter and receiver remain stationary and any Doppler effect is ignored.

Fig. 5 shows the BER performance comparison between the SC system and the PC/MC-FHSS system when multipath delay of the channel is small. The performance of systems, using or not using FHSS, is compared as well. The parameters employed in the simulation are at the top of the figure. Because of the fast hopping and frequency diversity combination, the BER performance of the SC-FHSS system is much better than the SC system over this multipath fading channel. For example, at a BER of 10^{-5}, the SNR of the SC-FHSS system is only 2 dB, which demonstrates the robust characteristic of the FHSS system while the SC system shows the error floor in this multipath fading channel. And the BER performance of the PC/MC-FHSS system is much better than that of the PC/MC system. From Fig. 5, we observe that when the BER rate is at 10^{-5}, the SNR needed in PC/MC FHSS system is about 2.8 dB, which is slightly bigger than that needed in SC-FHSS system. Consider the simulation multipath delay is relatively smaller in this simulation, especially when compared them with the parameters of these systems, i.e. $\tau_1 = 4$ ms and $\tau_1 = 8$ ms while the time intervals of the symbol of the two system are 50 ms and 10 ms, respectively. We expected that with the increase of the multipath delay, the BER performance of the PC/MC FHSS system will be more stable than that of the SC-FHSS system because it has much larger time interval, which will mitigate the influence of the ISI. The simulation results showed in Fig. 6 prove the hypothesis further.

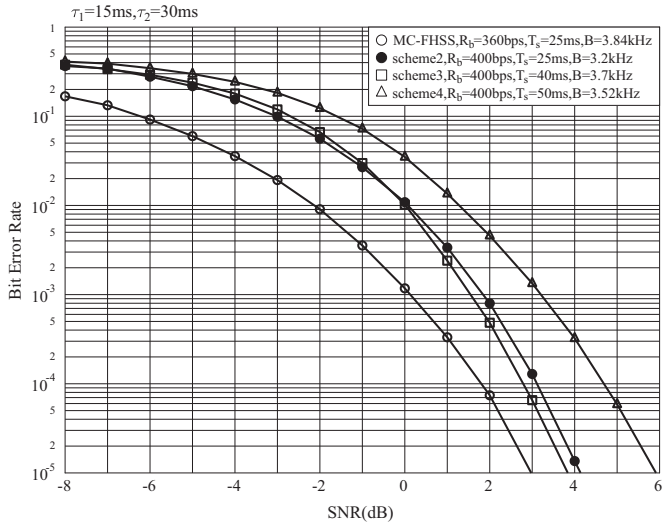

Fig. 7. BER performance comparison of the traditional MC-FHSS system and three schemes of the PC/MC-FHSS system, when communicating over 3-path fading channel, where $\tau_1 = 15$ ms and $\tau_2 = 30$ ms.

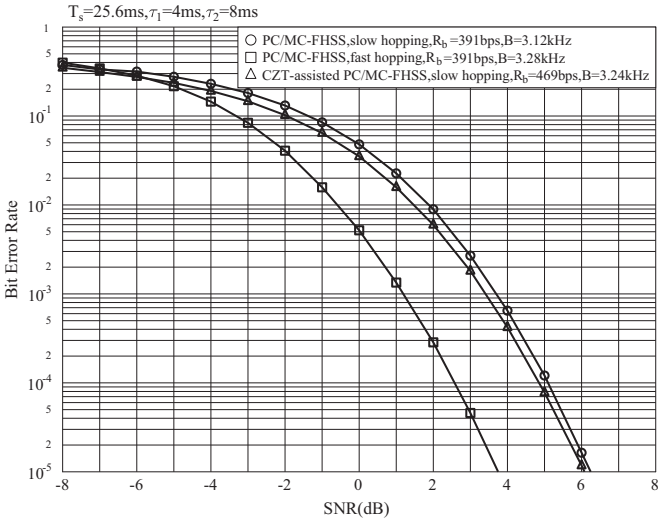

Fig. 8. BER performance comparison of the PC/MC-FHSS system and the CZT-assisted PC/MC-FHSS system, when communicating over 3-path fading channel, where $\tau_1 = 4$ ms and $\tau_2 = 8$ ms.

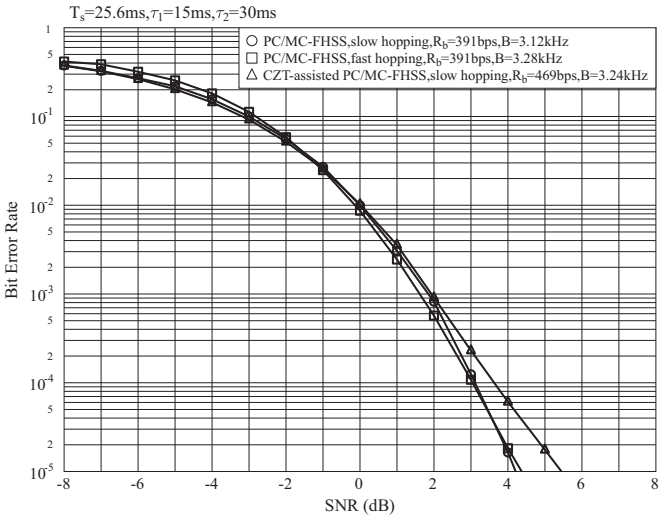

Fig. 9. BER performance comparison of the PC/MC-FHSS system and the CZT-assisted PC/MC-FHSS system, when communicating over 3-path fading channel, where $\tau_1 = 15$ ms and $\tau_2 = 30$ ms.

Fig. 6 shows the BER performance of the system discussed in Fig. 5 when large delay causes more serious frequency-selective fading. We observe that, the PC/MC-FHSS system significantly outperforms other systems. Error floors exist because of the serious multipath interference in the SC systems. Additionally, when we compare the BER performance of the PC/MC-FHSS system (see Figs. 5 and 6), we observe that it changes slightly and to some extent, the results of the simulations show that the proposed PC/MC-FHSS system is more robust over the large multipath fading channels. The results in Fig. 6 also shows that under this large delay multipath channel, the BER performance of the PC/MC-FHSS system is better than that of the SC-FHSS system.

Fig. 7 shows the BER performance comparison between the traditional MC-FHSS system and the three schemes of the PC/MC-FHSS system; other parameters employed in this simulation are shown at the top of the figure. The BER performance of the scheme 2 and scheme 3 are almost same, and both much better than the BER performance of the scheme 4. The main difference between these three schemes is the parameters such as M and R, as shown in Table 4. Based on PC theory, if one subcarrier of R subcarriers is detected incorrectly, the corresponding symbol (including K bits) may change dramatically. The BER performance will decrease with the increment of M and R. This decrease in performance is the main drawback of the PC/MC-FHSS system. Considering that all these three themes have the same data rate but occupying different bandwidth, it is a sensible to choose scheme 2 rather than the other two schemes over this kind of multipath channel. At a BER of 10^{-5}, the SNR of the MC-FHSS system is about 3 dB, while the SNR of the scheme 2 and scheme 3 is about 4 dB. But we should notice that the data rate of the MC-FHSS system is only 360 bps which is lower than that of the scheme 2 and scheme 3. And the bandwidth of the MC-FHSS system is 3.84 kHz which is the biggest one shown in Fig. 7. All these results show that the proposed PC/MC-FHSS system exhibits superior performance – especially under serious multipath interference conditions. In addition, the proposed PC/MC-FHSS system achieves a higher data rate than the MC-FHSS system, as well as the SC-FHSS system.

Fig. 8 shows the BER performance comparison between the PC/MC-FHSS systems and the CZT-assisted PC/MC-FHSS system, and the systems using fast and slow hopping mode are compared as well.The detailed parameters are shown in Tables 3, 4 and 5. And other parameters employed in the simulation are shown in the figure. In order to compare the fast hopped and slow hopped PC/MC-FHSS system at the same data rate level, we modify the parameters of the scheme 2 and change the symbol interval from $T_s = 25$ ms to $T_s = 25.6$ ms. From Fig. 8 we observe that the performance of the CZT-assisted PC/MC-FHSS system is similar to that of the PC/MC-FHSS system when working in the slow hopping mode, even though the data rate of the CZT-assisted PC/MC-FHSS system is 469 bps which is much faster than the data rate of the PC/MC-FHSS system. Furthermore, the bandwidths of the two schemes are almost identical. As shown in Fig. 8, the performance of the fast hopping PC/MC-FHSS system is the best because the diversity gain achieved by the fast hopping resists the narrowband interference. For example, at a BER of 10^{-5}, the SNR needed in the fast hopping PC/MC-FHSS system is only 3.6 dB, which is at least 2.4 dB lower than that of the other two systems.

Fig. 9 shows the BER performance of the system when the second and third path delays are 15 ms and 30 ms, respectively. We observe that, as the delay time τ increases, the performance of the PC/MC-FHSS system working in the fast hopping mode decreases slightly. For example, in Fig. 8, at a BER of 10^{-5}, the SNR

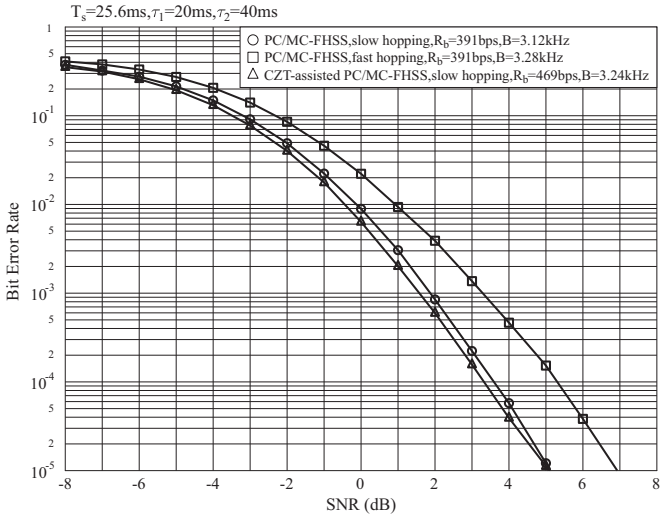

Fig. 10. BER performance comparison of the PC/MC-FHSS system and the CZT-assisted PC/MC-FHSS system, when communicating over 3-path fading channel, where $\tau_1=20$ ms and $\tau_2=40$ ms.

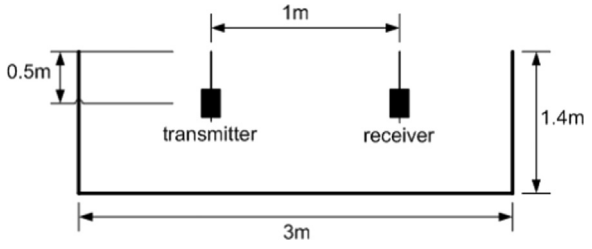

Fig. 11. The schematic diagram of Pool experiment.

needed is about 3.6 dB. While in Fig. 9, the needed SNR is about 4.2 dB. Similar results of the CZT-assisted PC/MC-FHSS system can be observed. In Fig. 8, at a BER of 10^{-5}, the needed SNR of the CZT-assisted PC/MC-FHSS system is about 6 dB, while in Fig. 9, it decreases to 5.5 dB. But the BER performance of the slow hopping systems changes rapidly. For example, in Fig. 9, when the BER of the slow hopping system is 10^{-5}, the SNR is about 4.2 dB. But in Fig. 8, the SNR needed at the same BER performance is about 6.0 dB. One the one hand, these results show that the proposed systems are robust over serious multipath fading channel. On the other hand, we consider that one reason for the BER performance increasing is the relationship between the parameters of the proposed systems and the parameters of the multipath channels, i.e., the symbol interval 25.6 ms and the delay of the second and third path $\tau_1=15$ ms and $\tau_2=30$ ms, respectively. Under these circumstances, the multipath maximum delay is close to the symbol interval. In order to demonstrate the performance of the proposed systems further, another simulation was made. As shown in Fig. 10, as the delay of channel increasing, such as $\tau_1=20$ ms and $\tau_2=40$ ms, the BER performance of the PC/MC-FHSS system which works in the fast hopping mode decreases. For example, at a BER of 10^{-5}, the needed SNR is about 7 dB. When compared it with that in the Fig. 9, we observe that the large delay causes loss of 2.8 dB at the BER of 10^{-5}. But when compare the BER performance of the PC/MC-FHSS system which work in slow hopping mode shown in Figs. 9 and 10, we observe that the performance decreases slightly. for example, at a BER of 10^{-5}, the SNR needed is about 4.2 dB in Fig. 9 but 5 dB is needed in Fig. 10. In contrast, the BER performance of the CZT-assisted PC/MC-FHSS system increase a bit. At a BER of 10^{-5}, when the delay is $\tau_1=20$ ms and $\tau_2=40$ ms, the needed SNR about 5 dB. While when the delay is smaller, i.e. $\tau_1=15$ ms and $\tau_2=30$ ms, the SNR is about 5.5 dB at the same BER. All these simulation results show that, to some extent, the proposed CZT-assisted PC/MC-FHSS system is more robust than the PC/MC-FHSS system especially under the serious frequency-selective fading circumstances.

Table 6
Results of pool experiment.

Scheme	SNR (dB)	BER	scheme	SNR (dB)	BER
Single-carrier	5	$<7.14e-4$	Scheme1	5	$2.8e-3$
Single-carrier	0	$<7.14e-4$	Scheme1	0	$6.0e-3$
Single-carrier	−2	$<7.14e-4$	Scheme1	−2	$8.7e-3$
Single-carrier	−5	$5.1e-4$	Scheme1	−5	$3.5e-2$
Scheme2	5	$<7.14e-4$	Scheme3	5	$<7.14e-4$
Scheme2	0	$1.4e-3$	Scheme3	0	$9.8e-3$
Scheme2	−2	$2.6e-3$	Scheme3	−2	$1.4e-2$
Scheme2	−5	$8.5e-2$	Scheme3	−5	$1.6e-1$
Scheme 5	5	$1.5e-4$	CZT-assisted	5	$2.09e-3$
Scheme 5	0	$8.3e-4$	CZT-assisted	0	$2.16e-2$
Scheme 5	−2	$1.3e-3$	CZT-assisted	−2	$3.5e-2$
Scheme 5	−5	$4.6e-2$	CZT-assisted	−5	$8.5e-2$

4. Pool experiment and result analysis

In this section, the proposed CZT-assisted PC/MC-FHSS system is verified by pool experiments. The size of Xiamen University's pool is 4.6 m × 3.0 m × 1.4 m. Because the size is not very large, and the walls and bottom are covered with ceramic tiles, serious multipath interference exists when an acoustic signal is transmitted from one point to another. The transmitter and receiver transducers are fixed at a depth of 0.5 m under the surface. The diagram of the experimental scene is shown in Fig. 11. For comparison, the BER performance results of the SC-FHSS system and the PC/MC-FHSS system are also shown in Table 6. The parameters of the systems are shown in Tables 1, 4 and 5. And the SNR of the received signal is relevant to the transmission distance and transmitting power.

Fig. 12 shows the CIR of the UWA channel in Pool. From Fig. 12 we see that the maximum delay of multipath transmission is about 10 ms. Under this circumstance, taking advantage of frequency diversity at the receiver, the performance of a SC-FHSS system is better than that of scheme 1, with the identical data rate of 200 bps. We observe from Table 6 that the BER of the SC system is on the order of 10^{-4}. When the data rate is 400 bps, from the results, we observe that the BER performance of scheme 2 and scheme 3 is almost identical at the high SNR, for example, when SNR is 5 dB and 0 dB. However, when the SNR decreases, i.e. the SNR is −2 dB, the BER performance of scheme 2 is better than that of the scheme 3, because in scheme 3, $M=37$ and $R=4$, which are bigger than scheme 2. Based on PC theory, when transmitted under the same circumstances, as M and R increase, any bit error will worsen the system's performance. Comparing the scheme 5 with scheme 2, we find the performance of the scheme 5 is almost identical to that of the scheme 2. Since the maximum multipath delay of the Pool is about 10 ms, the symbol intervals of the scheme 2 and scheme 5 (i.e. 25 ms and 25.6 ms, respectively) are large enough to resist the ISI. Furthermore, on the one hand, the frequency diversity gain is obtained by fast hopping in scheme 5. On the other hand, since the bandwidth of the system is limited, the fast hopping mode makes the interval of the subcarrier in scheme 5 decreased in half which adversely affect the effect of the frequency hopping. From the comparison between CZT-assisted PC/MC-FHSS and scheme 2, we observe that the performance of the CZT-assisted system is worse than that of scheme 2. Because when CZT method is used, the signal's

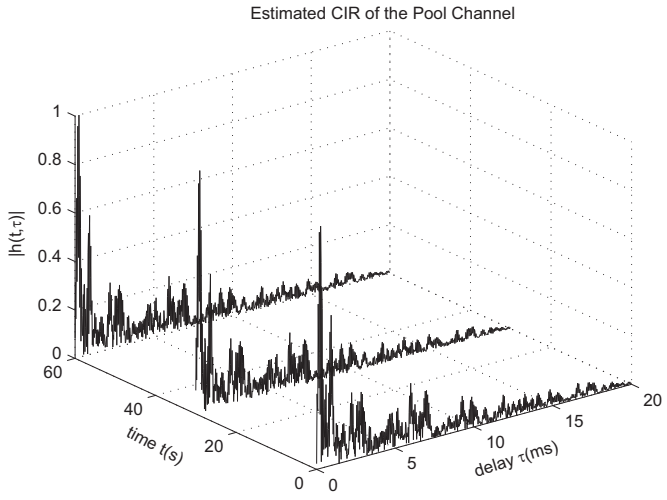

Fig. 12. The Channel Impulse Response of pool experiment.

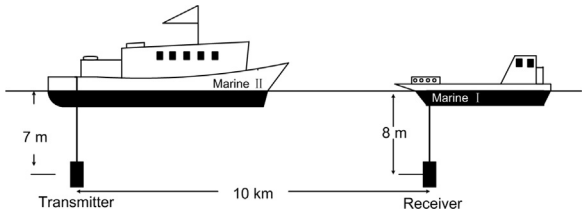

Fig. 13. The schematic diagram of outfield experiment.

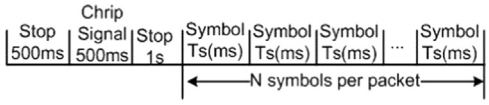

Fig. 14. Frame structure of the transmitted signal in outfield experiments.

minimum frequency interval is smaller than that of scheme 2, which leads to its weaker ability to resist multipath. However, the signal's data rate of the CZT-assisted PC/MC-FHSS system can reach 469 bps which is 69 bps higher than the scheme 2. All these results demonstrate the outstanding performance of the proposed CZT-assisted PC/MC-FHSS system under frequency selective fading circumstances.

5. Outfield experiment

Outfield experiments were conducted on September 22, 2012, and January 21, 2013, in Xiamen Port. The temperature of the sea water was 21.5 °C and 16 °C, respectively, and the state of the sea was almost same, it was slight, with wave heights about 0.5–1.25 m.

The diagram of the experimental setup is shown in Fig. 13. The transmitter was set on the ship of Marine II and was fixed 7 m beneath the surface where the water depth is 16 m. The emission direction of the transducer is omnidirectional. The receiver is set on Marine I ship and is fixed 8 m below the sea surface. In first outfield experiment, the scheme 2 and the scheme 3 were testified in the range of 10 km, and the scheme 3 was also verified in the range of 15 km. And there was only one receiver transducer that collected the signal at the receiver in the first experiment where the depths of the sea at the receiver side are about 15.5 m and 17 m in the range of 10 km and 15 km, respectively. In the second outfield experiment, the scheme 5 and CZT-assisted PC/MC-FHSS system were verified in the range of 10 km and there were 3 hydrophones fixed below the sea surface, the highest one was set 0.5 m beneath the surface, and the other two hydrophones were fixed at every 0.5 m interval. Fig. 14 is the frame structure of the transmitted signal. Parameters of the schemes and results are shown in Table 7.

Fig. 15 shows the CIR of the UWA channel when the communication distances are 10 km and 15 km, respectively. Fig. 15 also shows the time domain and frequency domain graphs of the received signal of scheme 3. The results of the 10 km-range experiment is given in the left column, and the results of the 15 km-range are given in the right column. From the two figures in the first row, we observe that the maximum multipath delay at different distances are 8 ms and 4 ms, respectively. The experiments were conducted in very shallow water, i.e. about 15 m. And during transmission, the acoustic signal encountered reflection off surface and bottom of the sea frequently, which make the energy of the acoustic signal faded quickly, only the signal transmitted over similar multipath channels could reach the receiver with certain energy which resulted that the maximum delay of the signal collected in 15 km range is smaller than that of the signal collected in 10 km range, while the state of the sea is similar. And from the two figures in the second row, we observe that it is difficult to distinguish the signal from the noise after such a long range transmission. Given that the transmitting electrical power are 115 W and 160 W at 10 km-range and 15 km-range, respectively. The estimated SNRs at receiver are 1.3 dB and 1.7 dB, respectively. We also observe from the figures of the third row that selective frequency fading exists in bandwidth of the proposed UWA communication system, between 4 kHz and 8 kHz and the higher the frequency of the signal, the more serious fading it will experience. Additionally, the power spectrum density (PSD) of the noise changes rapidly. The PSD of low-frequency noise is 10 dB/Hz higher than that of high-frequency noise, which is not in accordance with the presumed Gaussian White Noise.

Table 7 shows the experiment results. From Table 7, we observe that when the distance between the transmitter and the receiver is 10 km, the BER performance of scheme 2 is better than that of scheme 3. As shown in Fig. 15, since there exists frequency selective fading in the signal's bandwidth, the larger bandwidth of scheme 3 may lead to serious selective frequency fading. Additionally a large M and R of scheme 3 will result in a higher BER if the subcarrier frequency is wrongly detected based on PC theory. When the communication range is 15 km, the BER performance of scheme 3 is better than the same system working in the 10 km-range. From Fig. 15, we observe that PSD of the received signal in 15 km-range is different from that of the received signal in 10 km-range. High frequency signal faded obviously when compared with the signal collected in 10 km-range. Since we increased the transmitting electrical power at 15 km-range, the SNR of the received signal is 1.7 dB, which is higher than that of the 10 km-range, i.e., 1.3 dB. Another obvious difference observed from Fig. 15 is that the maximum delay in the 15 km-range is 4 ms, which is less than the 8 ms for 10 km-range. Decreasing ISI and higher SNR at the receiver when the communication distance is 15 km are reasons for the better BER performance.

When comparing the scheme 5 with the scheme 2, we observe that the BER of the scheme 5 is close to that of scheme 2. Since fast hopping was applied in the scheme 5, when working in the same communication distance, i.e., 10 km, the BER performance of the scheme 5 should be better than that of the scheme 2. We analyse the experiment to find out the reason. The two schemes were carried out in different outfield experiment, and the transmitting electrical power of the scheme 5 is (100 W) which is lower than that of scheme 2 (115 W). The estimated SNR of the scheme 5 is about −3 dB, which is much lower than that of the scheme 2

Table 7
Result of outfield experiment.

Scheme	Experiment date	Distance (km)	Bandwidth (kHz)	Transmitting electrical power (W)	Data rate (bps)	BER
Scheme 2	September 22, 2012	10	3.2	115	400	$1.5e-3$
Scheme 3	September 22, 2012	10	3.7	115	400	$1.0e-2$
Scheme 3	September 22, 2012	15	3.7	160	400	$6.8e-3$
Scheme 5	January 21, 2013	10	3.28	100	391	$3.6e-3$
CZT-assisted	January 21, 2013	10	3.36	100	469	$8.3e-3$

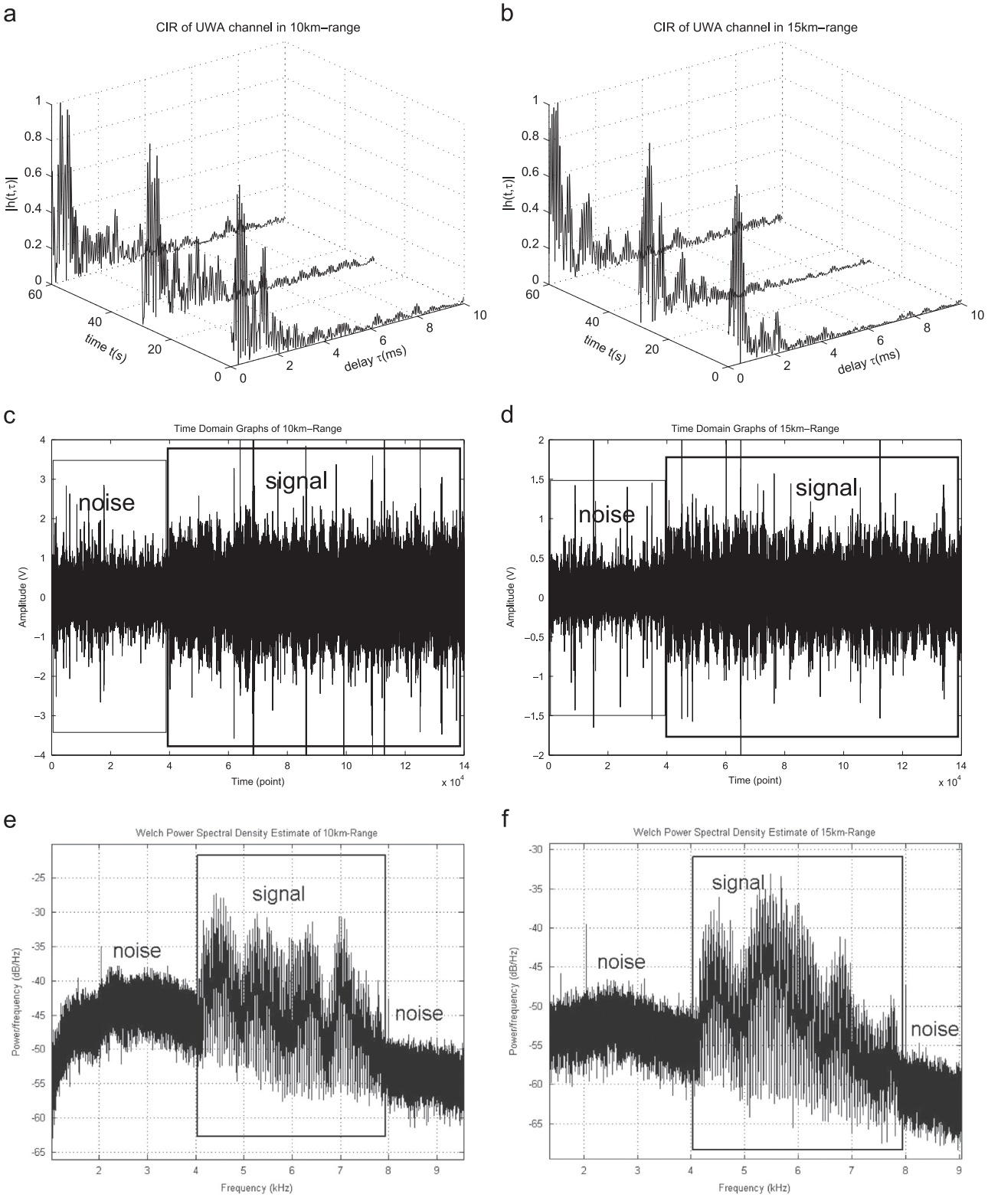

Fig. 15. The comparison of CIR and received signals of 10 km-range and 15 km-range, respectively. The left column is results of the 10 km-range, the transmitting electrical power is 115 W and the estimated SNR is about 1.3 dB. The right column is the results of the 15 km-range, the transmitting electrical power is 160 W and the estimated SNR is about 1.7 dB. (a) CIR of UWA channel in 10 km-range, (b) CIR of UWA channel in 15 km-range, (c) Time domain graph in 10 km-range, (d) Time domain graph in 15 km-range, (e) Frequency domain graph in 10 km-range, (f) Frequency domain graph in 15 km-range.

(1.3 dB). Additionally, in the second outfield experiment, though there were three hydrophones at receiver, only one of them had collected signal successfully. As we all know that the hydrophone has lower sensitivity than that of the transducer. All these demonstrate that, although their BERs are similar, the performance of the scheme 5 which takes advantage of the fast hopping should be more robust in UWA channel.

From Table 7, we also observe that the BER performance of the CZT-assisted PC/MC-FHSS system is also on the order of 10^{-3}, which is little worse than that of the scheme 5. This result is consistent with the result got from the pool. Since the multipath delay of this outfield experiment was only 8 ms which is on the same order of that in the pool. The estimated SNR of the CZT-assisted PC/MC-FHSS system is about -3 dB, which is similar to that of the scheme 5, but the data rate of the CZT-assisted system is 469 bps which is much higher than that of the scheme 5 (391 bps).

6. Conclusion

In this paper, a CZT-assisted PC/MC-FHSS UWA communication system was proposed. The structure of the system was presented, and the BER performance was invested through computer simulation, and pool and outfield experiments. Results show that when the distance of the communication is 10 km, the BER of the proposed system is about $8.3e-3$ with the data rate up to 469 bps.

Future research will address diversity combining and a new spectrum analysis method to improve the BER performance as well as to increase the data rate of the UWA communication system.

Acknowledgement

This research was funded by the Fundamental Research Funds for the Central Universities of China (No. 2010121062), the Natural Science Foundation of Fujian Province of China (No. 2013J01253) and the National Natural Science Foundation of China (Nos. 61301097 and 61301098).

References

Chaowu Zhan, X.H., Fang, Xu., 2013. Parallel combinatory multicarrier frequency hopped spread spectrum for long range and shallow underwater acoustic communications. In: WUWNet13, Kaohsiung, Taiwan.

Geng, X., Zielinski, A., 1995. An eigenpath underwater acoustic communication channel model. In: OCEANS95.MTS/IEEE. Challenges of Our Changing Global Environment Conference Proceedings, 2, pp. 1189–1196.

Guo, L., Yi, Q., Li, B., 2007. Parallel combinatory spectrum communication system based on r model combinatory [j]. Radio Commun. Technol. 33, 25–27.

Hu, Y., Jiao, B., 2005. Detection of underwater acoustic signals with dual-channel high-order spectrum. Tech. Acoust. 24, 65–69.

Huang, J., Chen, Y., Zhang, Q., Shen, X., Wang, F., 2005. Multi-frequency dpsk modulation for long-range underwater acoustic communication. In: Oceans 2005—Europe, 2, pp. 1074–1077.

Lam, W., Ormondroyd, R., 1998. A novel broadband cofdm modulation scheme for robust communication over the underwater acoustic channel. In: Military Communications Conference, 1998, MILCOM 98, Proceedings, IEEE, 478, vol. 1, pp. 128–133.

Liu, B., Yuan, F., Zhu, X., Cheng, E., 2012. Performance of underwater acoustic communication system based on fh-mfsk. In: 2012 2nd International Conference on Applied Robotics for the Power Industry (CARPI), pp. 934–936.

Rabiner, L.R, Schafer, R.W., 1969. The chirp z-transform. IEEE Trans. 486 Audio Electroacoust., 17, pp. 86–92.

Ran, M., Huang, J., Zhang, Q., Chen, Y., 2008. Self-differential joint frequency and phase modulation for long-range underwater acoustic communications. In: 9th International Conference on Signal Processing, 2008, ICSP 2008, pp. 1867–1870.

Shu, L., Shen, X., 2012. Research on shallow water acoustic communication based on frequency hopping. In: 2012 IEEE International Conference on Signal Processing, Communication and Computing (ICSPCC), pp. 392–395.

Stojanovic, M., 2008. Underwater acoustic communications: design considerations on the physical layer . In: Fifth Annual Conference on Wireless on Demand Network Systems and Services, 2008, WONS 2008, pp. 1 –10.

Stojanovic, M., Preisig, J., 2009. Underwater acoustic communication channels: propagation models and statistical characterization. IEEE Commun. Mag. 47, 84–89.

Stojanovic, M., Catipovic, J.A., Proakis, J.G., 1993. Adaptive multi-channel combining and equalization for underwater acoustic communications. J. Acoust. Soc. Am. 94, 1621–1632.

Tao, Y., Zhu, P., Xu, X., 2010. Dual-mode modulation based research of underwater acoustic modem. In: 2010 6th International Conference on Wireless Communications Networking and Mobile Computing (WiCOM), pp. 1 –3.

Wang, H., Pan, D., Shen, X., 2006. Research on two uwa frequency-hopped spread-spectrum communication methods in low sonic energy condition. In: 2006 IET International Conference on Wireless, Mobile and Multimedia Networks, pp. 1 –4.

Wang, D., Xu, R., Zheng, S., Xu, F., Hu, X., Liu, H., 2009. Research on base-band ofdm underwater acoustic communication system. In: 2009 1st International Conference on Information Science and Engineering (ICISE), pp. 2703 –2706.

Zhao, Z., Guo, S., 2010. An fhma acoustic communication system for multiple underwater robots. In: 2010 IEEE International Conference on Information and Automation (ICIA), pp. 1223–1228.

Zhu, J., Sasaki, S., 1991. Proposal of parallel combinatory spread spectrum communication system. In: Transactions of IEICE, J74-B-II, 2, pp. 207–214.